Numerical analysis of negative refraction of transverse waves in an elastic material

Anne-Christine Hladky, Jerome O. Vasseur, Bertrand Dubus, Bahram Djafari-Rouhani, D. Ekeom, B. Morvan

▶ **To cite this version:**

Anne-Christine Hladky, Jerome O. Vasseur, Bertrand Dubus, Bahram Djafari-Rouhani, D. Ekeom, et al.. Numerical analysis of negative refraction of transverse waves in an elastic material. Journal of Applied Physics, 2008, 104, pp.064906-1-6. 10.1063/1.2978379 . hal-00356649

HAL Id: hal-00356649
https://hal.science/hal-00356649v1

Submitted on 25 May 2022

HAL is a multi-disciplinary open access archive for the deposit and dissemination of scientific research documents, whether they are published or not. The documents may come from teaching and research institutions in France or abroad, or from public or private research centers.

L'archive ouverte pluridisciplinaire **HAL**, est destinée au dépôt et à la diffusion de documents scientifiques de niveau recherche, publiés ou non, émanant des établissements d'enseignement et de recherche français ou étrangers, des laboratoires publics ou privés.

Journal of Applied Physics

Numerical analysis of negative refraction of transverse waves in an elastic material

Cite as: J. Appl. Phys. **104**, 064906 (2008); https://doi.org/10.1063/1.2978379
Submitted: 23 April 2008 • Accepted: 18 July 2008 • Published Online: 18 September 2008

Anne-Christine Hladky-Hennion, Jérôme Vasseur, Bertrand Dubus, et al.


View Online


Export Citation

ARTICLES YOU MAY BE INTERESTED IN

Experimental demonstration of the negative refraction of a transverse elastic wave in a two-dimensional solid phononic crystal
Applied Physics Letters **96**, 101905 (2010); https://doi.org/10.1063/1.3302456

Negative refraction of acoustic waves in two-dimensional phononic crystals
Applied Physics Letters **85**, 341 (2004); https://doi.org/10.1063/1.1772854

Guiding and bending of acoustic waves in highly confined phononic crystal waveguides
Applied Physics Letters **84**, 4400 (2004); https://doi.org/10.1063/1.1757642

Lock-in Amplifiers up to 600 MHz
Zurich Instruments
Watch

© 2008 American Institute of Physics.

AIP Publishing

Numerical analysis of negative refraction of transverse waves in an elastic material

Anne-Christine Hladky-Hennion,[1,a)] Jérôme Vasseur,[1] Bertrand Dubus,[1] Bahram Djafari-Rouhani,[1] Didace Ekeom,[2] and Bruno Morvan[3]
[1]*Institut d'Electronique, de Microélectronique et de Nanotechnologie, UMR 8520 CNRS, Avenue Poincaré BP 60069, 59652 Villeneuve D'Ascq Cedex, France*
[2]*Microsonics 39, rue des Granges Galand, 37550 Saint-Avertin, France*
[3]*Laboratoire Ondes et Milieux Complexes (FRE CNRS 3102), Université du Havre, 76610 Le Havre, France*

(Received 23 April 2008; accepted 18 July 2008; published online 18 September 2008)

A numerical analysis of negative refraction process is reported using a phononic crystal with an elastic solid matrix. The phononic crystal considered in this study is made of a periodic arrangement of holes in aluminum. Dispersion curves are discussed and conditions for which negative refraction can appear are identified. These conditions are obtained for the transverse waves, whereas the longitudinal waves are evanescent. A calculation is performed with a prism shaped phononic crystal, and it clearly exhibits a negative refraction angle. Several analyses are provided with a view to characterize the wave going out of the phononic crystal. Finally, improvements, with respect to the impedance matching and index tuning, are discussed. © *2008 American Institute of Physics*. [DOI: 10.1063/1.2978379]

I. INTRODUCTION

There is a growing interest in the study of phononic crystals, which are composite materials made of a periodic arrangement of several elastic materials. Their dispersion curves may present, under certain conditions, absolute forbidden bands, e.g., frequency domains where the propagation of elastic wave is prohibited whatever the direction of propagation of the incident wave.[1] This property confers them potential applications in a wide frequency range.[2–4] If the presence of a band gap opens up potentialities for filtering applications, it is also possible to use unusual properties in the passbands of the dispersion curves. Following recent works on ultrarefractivity in photonic crystals,[5–7] researches are carried out on phononic crystals presenting a negative refraction that can focus acoustic waves.[8–16] These systems use particularities of dispersion curves, which can exhibit branches with negative slopes. Classically, when a wave propagates from one medium to another one, both its velocity and its direction change. For specific materials, a negative refraction can occur: the incident wave induces a wave in the phononic crystal, whose phase velocity and group velocity have opposite sign. Then, the Snell–Descartes relation at the interface implies a negative refraction angle to the wave. This latter approach relies on the Bragg scattering of the acoustic waves by the periodic array of inclusions. The potential applications of such devices are of main interest, in particular because they can reach the diffraction limit, i.e., the resolution can be smaller than half-wavelength, as previously highlighted in photonic crystals.[6]

Recent works on negative refraction of acoustic waves are devoted to phononic crystals made of solid inclusions in a fluid matrix. This paper reports numerical results on negative refraction of elastic transverse waves that can occur in simple phononic crystals with an elastic matrix (periodic arrangement of holes in aluminum). After recalling briefly the methods of calculation in Sec. II, we present in Sec. III the dispersion curves of aluminum phononic crystals and identify the conditions under which the negative refraction can occur. Then, the wave propagating inside the phononic crystal and inducing a negative refraction is characterized in Sec. IV. In Sec. V, a prism shaped phononic crystal is considered and negative refraction of the device is underlined. Finally, limits and improvements of the device are discussed.

II. MODELS AND METHODS OF CALCULATION

A. Plane wave expansion method for bulk phononic crystals

We briefly recall the basic principles of the plane wave expansion (PWE) method applied for computing the band structures of bulk two-dimensional (2D) phononic crystals. In this paper, phononic crystals made of square lattice of cylindrical holes drilled in a solid matrix made of cubic aluminum are considered. The holes of infinite depth are assumed parallel to the z axis of the Cartesian coordinate system (O,x,y,z). The intersections of the hole axes with the (xOy) transverse plane form a 2D periodic array and the nearest neighbor distance between holes is a. The 2D primitive unit cell contains one hole. The filling factor f of each hole is defined as the ratio between the cross-sectional area of a hole and the surface of the primitive unit cell (Fig. 1).

In the absence of an external force, the equation of propagation of the elastic waves in any composite material is given as

a)Electronic mail: anne-christine.hladky@isen.fr.

 © 2008 American Institute of Physics

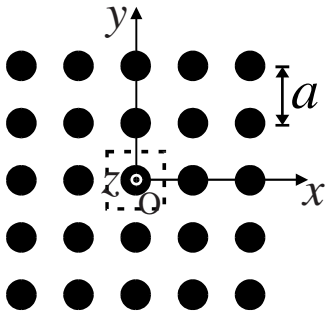

FIG. 1. Transverse cross section of the square array of cylindrical holes in a solid matrix. The holes are parallel to the z direction. The dotted lines represent the primitive unit cell of the 2D array.

$$\rho(\vec{r})\frac{\partial^2 u_i(\vec{r},t)}{\partial t^2} = \sum_{j,m,n} \frac{\partial}{\partial x_j}\left[C_{ijmn}(\vec{r})\frac{\partial u_n(\vec{r},t)}{\partial x_m}\right], \quad (1)$$

where $u_i(\vec{r},t)$ is a component $(i \equiv x,y,z)$ of the elastic displacement field $\vec{u}$. The elements C_{ijmn} $(i,j,m,n=1,\ldots,6)$ of the elastic stiffness tensor and the mass density ρ are periodic functions of the position vector $\vec{r}$. For bulk phononic crystals, i.e., assumed of infinite extent along the three spatial directions x, y, and z, *the elastic constants and the mass density do not depend on z*. Then taking advantage of the 2D periodicity in the (xOy) plane, the elastic constants and the mass density as well as the displacement field can be expanded in Fourier series. Inserting these Fourier transforms into Eq. (1) leads to a standard eigenvalue equation for which the sizes of the matrices involved depend on the number of 2D reciprocal lattice vectors $\vec{G}_{\|}$ taken into account in the Fourier series. This gives a set of eigenfrequencies ω for a given wave vector $\vec{k}_{\|}$. The numerical resolution of the eigenvalue equation is performed along the principal directions of propagation of the 2D irreducible Brillouin zone of the square array of inclusions. The PWE calculations reported in this paper were performed considering 169 two-dimensional $\vec{G}_{\|}$ vectors leading to a very good convergence of the PWE code.

In this paper, the lattice parameter of the square array of holes has been fixed to $a=0.77$ mm, but the radius R of the holes is varying, leading to varying filling factors of air in the phononic crystal. The three independent elements C_{11}, C_{44}, and C_{12} of the elastic stiffness tensor (expressed with the Voigt notation) and the mass density ρ of cubic aluminum used for the numerical calculations are $C_{11}=10.82\times10^{10}$ N/m^2, $C_{44}=2.85\times10^{10}$ N/m^2, $C_{12}=6.13\times10^{10}$ N/m^2, and $\rho_{\text{alu}}=2699$ kg/m^3. The transverse $V_{T\text{-alu}}$ and longitudinal $V_{L\text{-alu}}$ speeds of sound along the [100] crystallographic symmetry are equal to 3249 and 6331 m/s, respectively. Along the [110] crystallographic symmetry, they are, respectively, equal to 2948 and 6477 m/s. For alleviating numerical difficulties, the air inside the holes has been modeled with a low impedance medium.[17]

For the evaluation of the negative refraction capability of such solid matrix phononic crystal, the equifrequency surfaces (EFSs) were also drawn. They are deduced from the PWE dispersion curves calculated for different directions of propagation of the incident waves. Using a three-dimensional (3D) representation of the dispersion curves [i.e., $\omega(k_x,k_y)$], the EFSs are obtained by the intersection of the 3D dispersion curves with a horizontal plane, i.e., at fixed frequency.

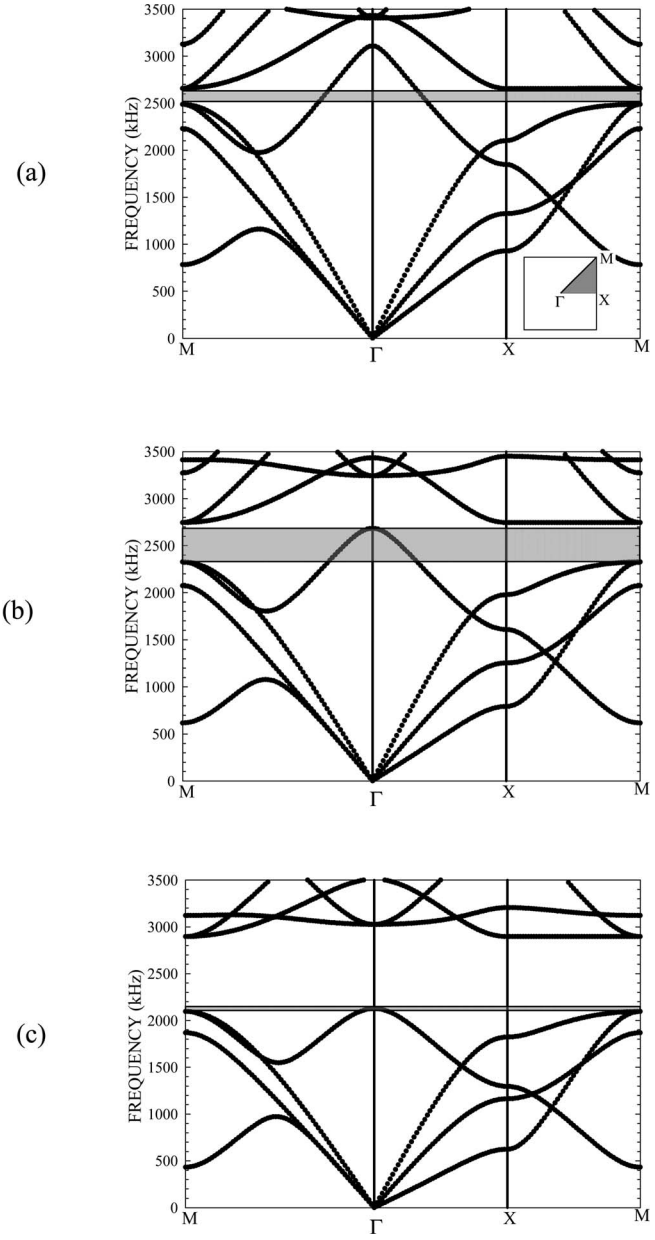

FIG. 2. PWE elastic band structures for the 2D phononic crystal made of a square array of holes in aluminum. The filling factor is (a) 40%, (b) 52%, and (c) 60%. The inset represents the first Brillouin zone ($M\Gamma XM$) of the square array. The gray areas correspond to the frequency range where negative refraction can occur.

B. Finite element method for bulk phononic crystals

Negative refraction of elastic waves has been also studied with the help of the finite element method (FEM), using the ATILA code,[18] and two different analyses have been carried out. In all cases, because the structure of interest is made of air cylinders of infinite depth drilled in a solid matrix, a 2D mesh is used, with a plane strain condition. The structure is meshed and divided into elements connected by nodes. In this study, isoparametric elements are used, with a quadratic

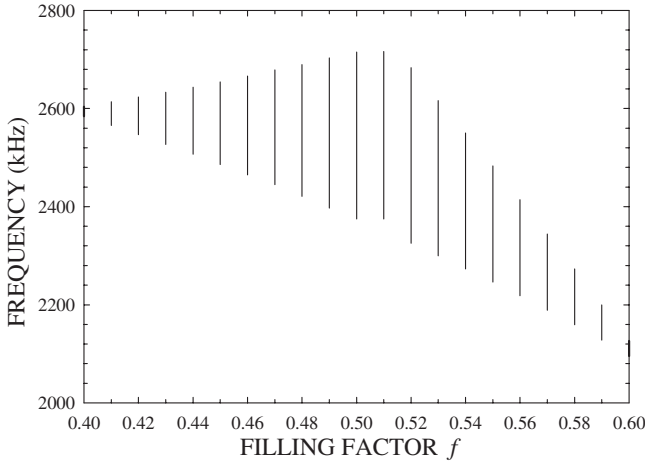

FIG. 3. Localization and width of the frequency range where negative refraction occurs vs the filling factor in the 2D phononic crystal.

interpolation along element sides. Moreover, due to the finite element formulation used here, the classical $\lambda/4$ criterion has to be verified, which states that the largest length of each element in a given mesh has to be smaller than a quarter of the wavelength in the material for the working frequency.

For the calculation of the displacement field at each node of the mesh at a given frequency, an harmonic analysis has been performed on the phononic structure. To avoid parasitic reflections on the boundaries of the mesh, a radiation condition is prescribed using a coupling between the FEM and the boundary element method (BEM). Thus, the medium outside the structure is supposed to be a semi-infinite medium. This condition, which relies on Green's functions, is only available for given geometries of the boundaries.[19]

With a view to study the propagation of elastic waves through the whole phononic crystal, a transient analysis is performed: the structure is submitted to given displacements on one part of the structure, with a view to excite either a longitudinal wave or a transverse wave. Then, a Fourier transform verifies that the given mode is well excited. For the transient analysis, a burst of five sinusoids is used at a given frequency. The mesh must be long enough before and after the phononic crystal to avoid parasitic reflections on the boundaries. Transient analysis is performed during 25 periods (T), with a $T/30$ time interval. Computations provide the displacement at each node and at each time interval. In particular, the displacements before and after the phononic crystal are studied and time-space diagrams are drawn. By applying a double Fourier transform on the diagrams, the calculations lead to a dual representation in the wave-number/frequency space, that is of interest for a comparison with the dispersion curves previously obtained with the PWE method.

III. DISPERSION CURVES

In this section, the phononic crystal made of a square array of circular holes in an aluminum matrix is considered. Figure 2 presents the dispersion curves in the first Brillouin zone, on the ΓXM path, for three different filling factors in the phononic crystal: $f=45\%$ ($R=0.29$ mm), $f=52\%$ ($R=0.313$ mm), and $f=60\%$ ($R=0.336$ mm). The results are rendered in terms of a frequency in kilohertz versus a reduced wave vector $\vec{K}=\vec{k}a/2\pi$. In each case, the dispersion curve exhibits one or several branches with a negative slope, i.e., the frequency is decreasing with increasing wave vector modulus. Negative refraction can occur if only one branch with a negative slope exists in a frequency range (this region is marked by the gray rectangles in Fig. 2). Figure 3 presents the variations in the frequency range where negative refraction can occur, as a function of the filling factor of air in the phononic crystal. It shows that the maximum frequency bandwidth (2320–2685 kHz) is obtained for 52% of air in the phononic crystal, corresponding to the dispersion curve displayed in Fig. 2(b). Considering a wave propagating on the ΓX path only, negative refraction can occur on a larger bandwidth (1977–2685 kHz), as observed in Fig. 2(b).

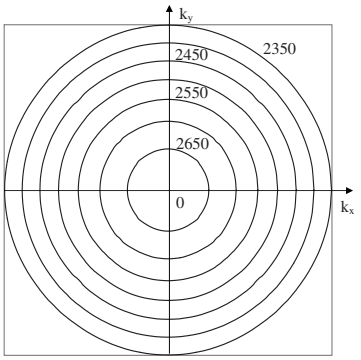

FIG. 4. EFS of the phononic crystal with 52% of air. Frequencies are varying from 2350 to 2650 kHz with 50 kHz step. The maximum values of k_x and k_y are 1.3 mm^{-1}.

Figure 4 presents the EFS for the phononic crystal with 52% of air for various frequencies (from 2350 to 2650 kHz with a 50 kHz step). They exhibit a quasicircular shape, with a decreasing radius with increasing frequency. That means that the wave vector of the elastic wave and the group velocity are antiparallel, whatever the propagation direction. The group velocity ($d\omega/dk$) can be determined from Fig. 4. It slowly decreases as the frequency increases (from $\sim$2200 m/s at 2350 kHz to $\sim$2000 m/s at 2550 kHz). The phase velocity in the phononic crystal V_{pc}, determined by the ratio ω/k, is presented in Fig. 5, on two different paths: ΓX (i.e., an angle of incidence of 0°) and ΓM (45°). Both paths give close results. The variations in the phase velocity are

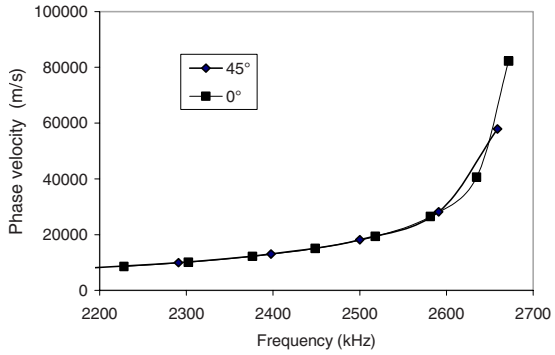

FIG. 5. (Color online) Variation in the phase velocity in the phononic crystal as a function of the frequency, for the branch with a negative slope.

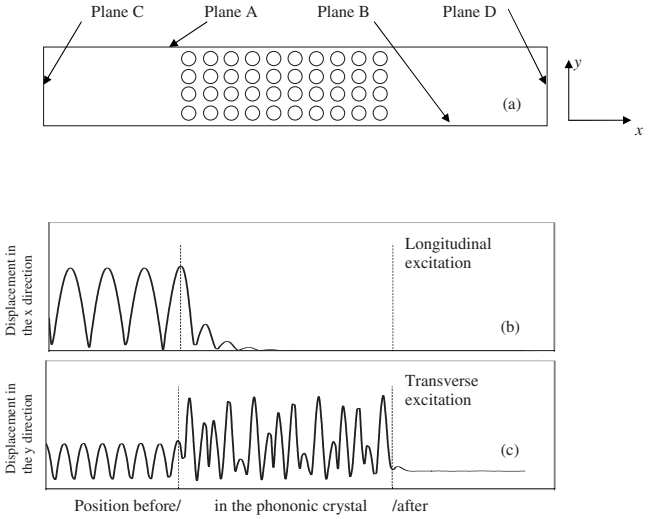

FIG. 6. (a) Schematic description of the calculated structure made of a phononic crystal slab sandwiched between two semi-infinite media. A periodic condition is applied on planes A and B. Excitation is applied on plane C. A FEM-BEM coupling is applied on planes C and D. (b) Variations in the amplitude of the displacement in the x direction as a function of the position when the excitation is a longitudinal force. (c) Variations in the amplitude of the displacement in the y direction as a function of the position when the excitation is a transverse force. The vertical dotted lines correspond to the edges of the phononic crystal slab. Amplitudes are normalized.

large, in particular at high frequency: it starts around ~8000 m/s at 2200 kHz and increases to ~30000 m/s at 2600 kHz. According to the Snell–Descartes law, the angle of negative refraction at the interface between a homogeneous medium and the phononic crystal depends on the incidence angle, on the phase velocity in the homogeneous medium and in the phononic crystal. Consequently, an optimal negative angle of refraction for a specific frequency requires to choose accurately the physical characteristics of the homogeneous medium and to know the phase velocity in the phononic crystal. To ensure that the rays emitted by a point source will converge to an image point, the velocities of both media (homogeneous medium and phononic crystal) should be equal.

IV. CHARACTERIZATION OF WAVES PROPAGATING THROUGH THE PHONONIC CRYSTAL

In this section, the phononic crystal with 52% of air is considered. In the frequency domain depicted with a gray area in Fig. 2(b), a single mode propagates through the phononic crystal. The dispersion curve associated with this mode exhibits a negative slope. In order to analyze the nature of this mode, we consider [see Fig. 6(a)] a structure made of a slab of air holes/aluminum phononic crystal (with a thickness of the order of ten periods) sandwiched between two homogeneous media constituted of bulk aluminum. A periodic condition is applied on planes A and B, thus the device is supposed to contain ten infinite rows of holes. The device is analyzed using the FEM. An incident plane wave is impinging the array at normal incidence, by prescribing a force on plane C. Either a longitudinal or a transverse harmonic force is applied, with a view to propagate a longitudinal or a transverse wave in the array. To avoid parasitic reflections on

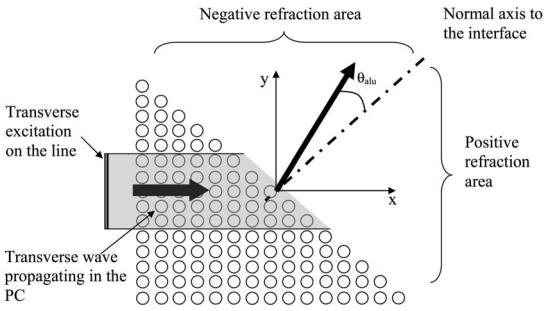

FIG. 7. Schematic description of the calculated structure with a view to reveal a negative refraction of transverse waves.

the boundaries of the mesh (planes C and D), a radiation condition is prescribed using a BEM representation.[19] Thus, the homogeneous media placed on both sides of the phononic crystal slab may be assumed as semi-infinite media. The displacement inside the phononic crystal is displayed in Figs. 6(b) and 6(c), when a longitudinal force and a transverse force are, respectively, applied on plane C. For the sake of simplicity, only the modulus of the displacement is displayed.

The frequency of the incident wave (2400 kHz) falls in the frequency domain where negative refraction may occur [see Figs. 2(b) and 3]. Figure 6(b) shows that, when a longitudinal force is applied on the left side of the structure, the displacement in the x direction of the longitudinal wave in the phononic crystal decreases and is approximately equal to 0 after 4 rows of holes. This result illustrates the presence of a band gap for the longitudinal wave at 2400 kHz. Stationary waves are observed between the excitation (plane C) and the phononic crystal. One can notice a total reflection of the wave. The standing wave ratio (SWR) is equal to 1. The minima are reaching zero periodically in front of the phononic crystal, and the amplitude of the displacement behind the phononic crystal is equal to 0.

When a transverse force is applied on the left side of the structure, a transverse wave is induced in the phononic crystal. The displacement in the y direction of the wave propagating behind the phononic crystal remains constant and is not equal to 0. One can notice that the displacement field inside the phononic crystal presents large variations, which are related to interferences. Once again, stationary waves take place between the excitation and the phononic crystal. In this case, the SWR is lower than 1 as the amplitude of the minima before the phononic crystal does not reach 0.

As a conclusion, Fig. 6 shows that the branch with a negative slope corresponds to a transverse mode, whereas the longitudinal waves are evanescent in this frequency range.

V. DEMONSTRATION OF NEGATIVE REFRACTION PROPERTY

The aim of this section is to demonstrate that the chosen phononic crystal exhibits a negative refraction for transverse waves. A calculation is then performed with a prism shaped phononic crystal (15×15 rows), as described in Fig. 7. The calculations are performed with the FEM.[18] The excitation is generated by a y displacement prescribed on a vertical line

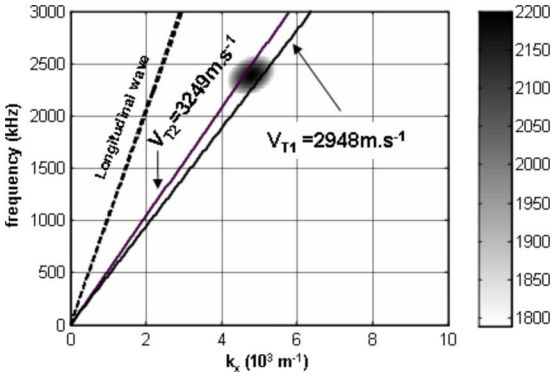

FIG. 8. (Color online) Amplitude of the y displacements of the incident signal in the (wave number/frequency) space along the x direction. The transverse and the longitudinal wave numbers, in the [100] and [110] directions, are plotted, respectively, in solid and dashed lines.

on the left part of the phononic crystal. A time analysis is carried out and the excitation corresponds to a burst made of five sinusoids. Central frequency is 2400 kHz. It is expected that the incident wave first impinges the phononic crystal at normal incidence along the ΓX path, then propagates inside the phononic crystal, and finally leaves the phononic crystal with an angle that reveals a negative refraction.

To verify that the excitation produces an incident transverse wave incident on the phononic crystal, the displacements in the y direction are recorded along a horizontal line, on the left part of the phononic crystal. Applying a time and a spatial fast Fourier transform (FFT), the signal gives the wavenumber versus the frequency (Fig. 8). It shows a spot on the figure: it falls between two lines, which slopes are the transverse wave velocities in aluminum in the [100] and [110] directions. The amplitude of the transverse wave is maximum at the excitation frequency. Longitudinal waves are not generated. In this frequency range negative refraction can occur, as previously observed in Fig. 2(b).

Figure 9 displays the amplitude of the displacement field at time $t=5\ \mu$s. During that duration, the lateral wave propagates through the phononic crystal and produces a transmitted wave. It shows that mechanisms inside the phononic crystal are more complex when it has an elastic matrix, because of the coexistence of longitudinal waves and transverse waves in a solid.

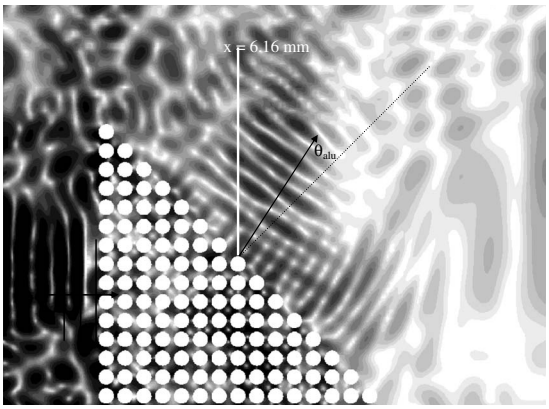

FIG. 9. Amplitude of the displacement field at $t=5\mu$s. The dotted line is the normal axis to the phononic crystal. The full black line shows that a negative angle is observed when the wave is leaving the phononic crystal.

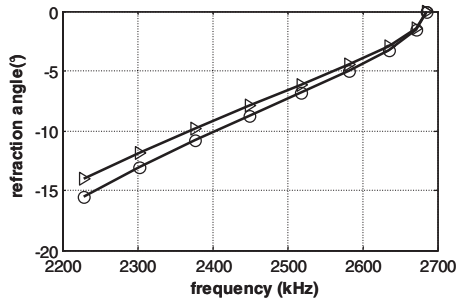

FIG. 10. Variations in the refraction angle as a function of the frequency, thanks to the Snell–Descartes law, using variations in the phase velocity from Fig. 5. The angle of incidence in the phononic crystal is equal to 45°. Two transverse wave velocities are considered in aluminum: $V_{T2}=3249$ m/s (circles) and $V_{T1}=2948$ m/s (triangles).

In Fig. 9, the normal axis of the phononic crystal is displayed and shows that the angle of the outgoing wave is negative. The theoretical value of the angle of refraction θ_{alu} can be easily deduced from the Snell–Descartes law. Considering that the wave in the phononic crystal reaches the second interface with an angle of incidence θ_{pc} equal to 45°, the Snell–Descartes relation gives then

$$\frac{\sin\ \theta_{\text{pc}}}{V_{\text{pc}}} = \frac{\sin\ \theta_{\text{alu}}}{V_{T\text{-alu}}}. \tag{2}$$

Considering the variations in the phase velocity inside the phononic crystal reported in Fig. 5, Fig. 10 presents the variations in the refraction angle at the interface between the phononic crystal slab and the homogeneous aluminum medium, θ_{alu} versus frequency. It is calculated using both transverse wave velocities in aluminum, in the [100] and in [110] directions, respectively, $V_{T1}=3249$ m/s and $V_{T2}=2948$ m/s. The larger difference (1°) between the refraction angles related to these two transverse waves appears in the lower part of the frequency band (2250 kHz). The shift decreases as the frequency increases. One can notice that the refraction angle is relatively small because the phase velocity in the phononic crystal is much larger than the velocity in bulk aluminum, as seen in Fig. 5. A more significant negative refraction process would occur if the refraction indices of both media (phononic crystal and bulk external elastic medium) were "tuned."[16] Ideally, if the refraction angle is equal to the incident angle, then all rays emitted by a point source will be focused at the same point.

The angle θ_{alu} can be extracted from the numerical simulation. From the displacements along the y direction where the wave is leaving the phononic crystal (at a position $x=6.16$ mm, the origin $x=0$ being located at the first interface of the phononic crystal), the identification of the propagating modes is performed in the dual space by applying a time and a spatial FFT (2D FFT). Thus, the y component of the wavenumber k_y versus the frequency is obtained and displayed in Fig. 11. The main spot is located around 2325 kHz and corresponds to a transverse wave leaving the phononic crystal. Thanks to the superposition of the theoretical values of the y component of the transverse wavenumber $[k_{\text{Ty}}=\omega\cos(45-|\theta_{\text{alu}}|)/V_{T\text{-alu}}$, ω being the angular frequency), one can estimate the refraction angle of the transverse wave: $\theta_{\text{alu}}=\sim$

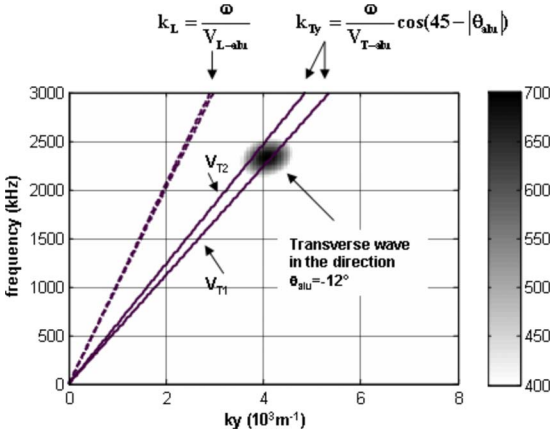

FIG. 11. (Color online) Amplitude of the displacement of the transmitted signal in the (wave number/frequency) space along the y direction. The projection along the y direction of the transverse wave numbers ($k_{Ty} = \omega \cos(45 - |\theta_{alu}|)/V_{T\text{-alu}}$) transmitted through the phononic crystal at a negative refraction angle $\theta_{alu} = -12°$ is plotted in dashed lines for the two wave velocities, in the [100] and [110] directions. Longitudinal wave numbers, in the [100] and [110] directions, are plotted in solid lines.

−12°. This value is in good agreement with the theoretical one (Fig. 10) deduced from the Snell–Descartes relation (between −11.2° and −12.4° at $f = 2325$ kHz) and with the result displayed in Fig. 9. No other spot corresponding to the longitudinal wave in aluminum in the [100] and [110] directions is observed in Fig. 11. Similar numerical results are obtained considering the displacement in the x direction on a vertical line.

Finally, the amplitude of the outgoing wave is very low in comparison with the incident wave, as previously observed in Fig. 6(c): a part of the incident wave is reflected at the interfaces between the bulk aluminum and the phononic crystal. Therefore, the acoustic impedances of both mediums (bulk aluminum and phononic crystal) could be adapted for a better transmission of the waves at the interfaces between the different media.

VI. CONCLUSION AND PERSPECTIVES

The numerical analysis of negative refraction process has been reported using a phononic crystal with an elastic matrix. Negative refraction is obtained for transverse waves. Further investigations are performed by changing the symmetry of the phononic crystal. Future works will concern the adaptation of impedances of both media, to ensure the transmission of the waves between the phononic crystal and the external elastic medium. Finally, the refraction indices of these media have to be tuned. This condition is particularly important as focusing is one of the potential applications of the device.

[1]For a is a comprehensive list of references on phononic crystals, see the Phononic Crystal database at http://www.phys.uoa.gr/phononics/PhononicDatabase.html
[2]R. Martínez-Sala, J. Sancho, J. V. Sánchez, V. Gómez, J. Llinares, and F. Meseguer, Nature (London) **378**, 241 (1995).
[3]A. Khelif, A. Choujaa, S. Benchabane, V. Laude, and B. Djafari-Rouhani, Proceedings of the 2004 IEEE Ultrasonics Symposium, pp. 654–657.
[4]J. O. Vasseur, A. C. Hladky-Hennion, P. A. Deymier, B. Djafari-Rouhani, F. Duval, B. Dubus, and Y. Pennec, J. Appl. Phys. **101**, 114904 (2007).
[5]J. M. Lourtioz, *Photonic Crystals: Towards Nanoscale Photonic Devices* (Springer, New York, 2005).
[6]J. B. Pendry, Phys. Rev. Lett. **85**, 3966 (2000).
[7]C. Croënne, N. Fabre, D. V. Gaillot, O. Vanbésien, and D. Lippens, Phys. Rev. B **77**, 125333 (2008).
[8]J. H. Page, A. Sukhovich, S. Yang, M. L. Cowan, F. Van Der Biest, A. Tourin, M. Fink, Z. Liu, C. T. Chan, and P. Sheng, Phys. Status Solidi B **241**, 3454 (2004).
[9]X. Zhang and Z. Liu, Appl. Phys. Lett. **85**, 341 (2004).
[10]S. Yang, J. H. Page, Z. Liu, M. L. Cowan, C. T. Chan, and P. Sheng, Phys. Rev. Lett. **93**, 024301 (2004).
[11]C. Qiu, X. Zhang, and Z. Liu, Phys. Rev. B **71**, 054302 (2005).
[12]M. Ke, Z. Liu, C. Qiu, W. Wang, J. Shi, W. Wen, and P. Sheng, Phys. Rev. B **72**, 064306 (2005).
[13]J. Li, Z. Liu, and C. Qiu, Phys. Rev. B **73**, 054302 (2006).
[14]L. Feng, X.-P. Liu, M.-H. Lu, Y.-B. Chen, Y.-F. Chen, Y.-W. Mao, J. Zi, Y.-Y. Zhu, S.-N. Zhu, and N.-B. Ming, Phys. Rev. B **73**, 193101 (2006).
[15]L. Feng, X.-P. Liu, M.-H. Lu, Y.-B. Chen, Y.-F. Chen, Y.-W. Mao, J. Zi, Y.-Y. Zhu, S.-N. Zhu, and N.-B. Ming, Phys. Rev. Lett. **96**, 014301 (2006).
[16]A. Sukhovich, L. Jing, and J. H. Page, Phys. Rev. B **77**, 014301 (2008).
[17]J. O. Vasseur, P. Deymier, B. Djafari-Rouhani, Y. Pennec, and A.-C. Hladky-Hennion, Phys. Rev. B **77**, 085415 (2008).
[18]ATILA Finite Element Code for Piezoelectric and Magnetostrictive Transducers Modeling, Version 5.2.1, User's Manual, ISEN, Acoustics Laboratory, Lille, France, 2002.
[19]D. Ekeom, A. Volatier, and B. Dubus, Proceedings of the 2006 IEEE Ultrasonics Symposium, pp. 1474–1477.